# Altered spike dynamics drives immune evasion of SARS-CoV-2

Hasan Uğurlu[1], Petja Salminen[1], Meng Yuan[2], Riku Fagerlund[1], Anna R. Mäkelä[1], Eva Žusinaite[3], Tapio Kesti[1], Ilona Rissanen[4], Andres Merits[3], Ian A. Wilson[2] & Kalle Saksela*[1,5]

[1] Department of Virology, University of Helsinki, Helsinki, Finland

[2] Dept. of Integrative Structural and Computational Biology, The Scripps Research Institute, La Jolla, CA 92037, USA

[3] Institute of Bioengineering, University of Tartu, Tartu, Estonia.

[4] Institute of Biotechnology, Helsinki Institute of Life Science HiLIFE, University of Helsinki, Helsinki, Finland.

[5] HUS Diagnostic Centre, HUSLAB, Clinical Microbiology, Helsinki University Hospital, Helsinki, Finland.

*corresponding author

**SUMMARY**

Rapid viral escape from protective immunity has been an unwanted hallmark of the COVID-19 pandemic. This escape has been attributed to mutations in critical neutralizing antibody epitopes mainly in the receptor binding domain (RBD) of the viral spike glycoprotein. Here we show that this notion is incomplete. We found that several broadly neutralizing human antibodies isolated over the past years retain an almost undiminished capacity for inhibitory targeting of RBDs of recent highly immunoevasive SARS-CoV-2 strains. Likewise, human sera collected during the pre-Omicron era from persons immunized with original Wuhan-based vaccines were found to contain abundant neutralizing activity targeted against the RBDs of modern Omicron variants. However, this unexpected neutralization sensitivity was observed only when these RBDs were incorporated into a mismatched spike protein backbone, whereas the corresponding native Omicron spike proteins were highly resistant against the same panel of antibodies and human sera. We conclude that changes occurring outside of the RBD and leading to altered conformational dynamics of the spike protein have played a key part in the viral evolution enabling SARS-CoV-2 to escape from neutralizing antibodies that target highly conserved cryptic RBD epitopes.

## INTRODUCTION

The SARS-CoV-2 pandemic has resulted in 776 million confirmed cases of COVID-19 and 7 million deaths as of October 2024 [1]. Rapid sequence evolution involving the neutralizing epitopes in the viral spike glycoprotein during the ongoing pandemic has undermined the ability of the available vaccines to protect from infection as well as the utility of the approved therapeutic antibodies in treating COVID-19 patients [2]. The magnitude of this challenge escalated upon the emergence of the Omicron variant reported in South Africa in November 2021, and the spread of its subvariants [3-8].

Approximately 90% of all neutralizing antibodies (NAb) against SARS-CoV-2 target the receptor binding domain (RBD) of the spike protein [9, 10]. The majority of NAbs in COVID-19 patients and the first generation of therapeutic antibodies are specific for the receptor-binding motif (RBM) in the RBD, and act by preventing the RBD from engaging with the host receptor ACE2. However, RBM-binding antibodies are sensitive to SARS-CoV-2 sequence variation and tend to lose affinity against emerging variants (see e.g. ref. 3 [3]).

By contrast, many NAbs that bind to conserved RBD regions outside of the RBM show broad neutralizing potency against divergent SARS-CoV-2 variants[11-13] as well as other sarbecoviruses, including SARS-CoV-1, and related animal viruses regarded as potential zoonotic threats. Such broadly neutralizing antibodies (bnAbs) typically target so-called cryptic sites in the RBD core region, which are occluded in the predominating closed conformation of the spike trimer where all or two out of the three RBDs are in “down-orientation” [14]. In some cases, cryptic sites require even greater opening and rotation of the RBDs to accommodate antibody binding, e.g. CR3022 [15] and S2H97 [16]. However, the inhibitory potency of these bnAbs is typically lower in comparison to RBM-targeting NAbs [4, 8, 17].

While the escape of emerging new SARS-CoV-2 variants from neutralization by RBM-targeting NAbs is driven by the accumulation of amino acid changes that alter their target epitopes, it is less well understood how viral evolution may have contributed to the relative resistance of SARS-CoV-2 variants against bnAbs. Here we report that, in comparison to the ancestral SARS-CoV-2 strain, most of the Omicron lineage variants show markedly increased bnAb resistance to pre-existing immunity. However, in contrast to evasion from RBM-binding NAbs, escape from the cryptic site-targeting bnAbs reported here does not appear to be driven primarily by target epitope loss but instead by altered conformational dynamics of the spike protein arising from mutations outside of the RBD region.

## RESULTS

We examined the literature on bnAb clones obtained from COVID-19 patients and vaccinees to assemble a panel of structurally and functionally well-characterized antibodies. We did not include antibodies reported to have very low neutralization potencies, and also excluded bnAbs whose binding footprints substantially overlapped with the ACE2 binding interface. Accordingly, we chose to recombinantly express six prominent bnAbs, namely COVA1-16 [18], 10-28 [14], 10-40 [14], 2-36 [19], C022 [20], and S2H97 [16], five (COVA1-16, 10-28, 10-40, 2-36, C022) of which target the highly conserved class IV/CR3022 site [13] using a YYDxxG motif in their CDR H3 (except 10-28), and one targeting the

conserved site V (S2H97) in the RBD. A compilation of the structures of these antibodies in complex with RBD and survey of the associated binding footprints is provided in Figure S1.

The neutralization capacity of these antibodies was tested using a panel of pseudoviruses carrying spike glycoproteins of the prototypic B.1 virus ("Wuhan-D614G" in the following) or 10 diverse Omicron variants, including BA.1, BA.2, BA.4/5, BA.2.75 (Centaurus), XBB (Gryphon), BF.7 (Minotaur), BQ.1.1 (Cerberus), BU.1, and XBB.1.5 (Kraken), and EG.5.1 (Eris).

All six antibodies could efficiently neutralize Wuhan-D614G with $IC_{50}$ values in agreement with the published data (Figure 1). By contrast, the Omicron variants were considerably more resistant to these antibodies, showing $IC_{50}$ values typically more than one and, in many cases, more than two orders of magnitude higher than for Wuhan-D614G.

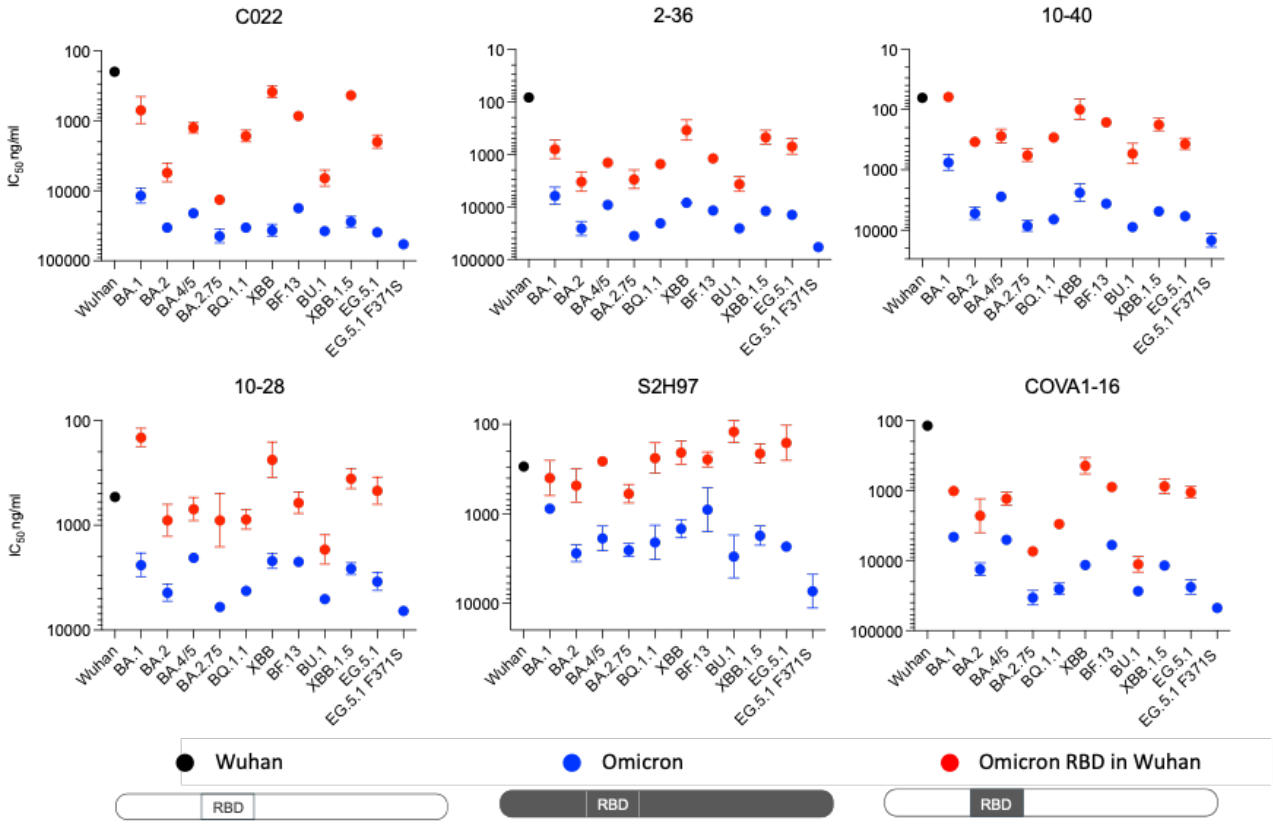


***Figure 1.*** *Neutralization by six prominent bnAbs of pseudoviruses carrying a spike protein from the ancestral Wuhan-D614G virus (black dot) or from 10 different Omicron variants (blue dots) or a chimeric spike containing the RBD (residues 330-529) of the same Omicron variants in the Wuhan-D614G backbone (red dots). Neutralization assays were repeated two or more times independently in duplicates. The averages and standard deviations of representative assays are shown. The original data are provided as a Source Data file.*

Increased resistance against neutralization by RBD-binding antibodies is thought to be due to abrogated binding capacity of these antibodies caused by RBD mutations that have accumulated during the immune escape-driven SARS-CoV-2 evolution [3, 6, 8, 17, 21-24]. To further explore this concept, we constructed pseudoviruses carrying chimeric spike proteins containing the RBDs from the

neutralization-resistant Omicron variants placed into the backbone of the Wuhan-D614G strain. Surprisingly, we observed that these Omicron RBDs did not transfer the resistant phenotype to Wuhan-D614G spike and, instead, the resulting chimeric spike proteins were remarkably easy to neutralize when compared to the corresponding native Omicron spike proteins. For example, in contrast to the poor neutralization of the XBB pseudovirus, the virus carrying a chimeric Wuhan-D614G spike with XBB RBD became even more easy to neutralize for some antibodies than the native Wuhan-D614G virus (Figure 1). Of note, all of these sensitive chimeric viruses carried a hydrophobic (L or F) substitution of RBD residue S371, which has been implicated as a cause for resistance against several classes of neutralizing antibodies [22, 23]. To further test the role of this residue, we introduced a F371S mutation into of EG.5.1 spike to restore a Wuhan-like serine residue in this position. This mutation did not sensitize EG.5.1 to our panel of bnAbs, and EG.5.1-F371S was even more resistant to neutralization than the native EG.5.1 spike (Figure 1).

These results prompted us to study sera from individuals immunized with the original Wuhan-based vaccines in the pre-Omicron era. In addition to XBB, BQ.1.1, XBB.1.5, and EG.5.1 used in the studies shown in Fig. 1, another more recent Omicron variant JN.1 was included in this experiment. Five vaccine sera collected before February 2022 were tested and found to have strong neutralizing activity against the ancestral Wuhan-D614G virus ($ID_{50}$ titers ranging between 5382 – 442; Figure 2). By contrast and as expected based on the well-documented immunoevasive potential of these viruses [3, 7, 25-27], the neutralization potency of these sera against the five tested Omicron variants was poor, showing titers that were more than an order of magnitude lower than observed for Wuhan-D614G and, in more than half of the cases, too low to be accurately determined. In agreement with the literature [9, 10], the neutralizing capacity of these sera was almost completely mediated by RBD-targeted antibodies, as 99% to 93% of this activity could be removed by immunodepletion with beads coated with recombinant RBD protein.

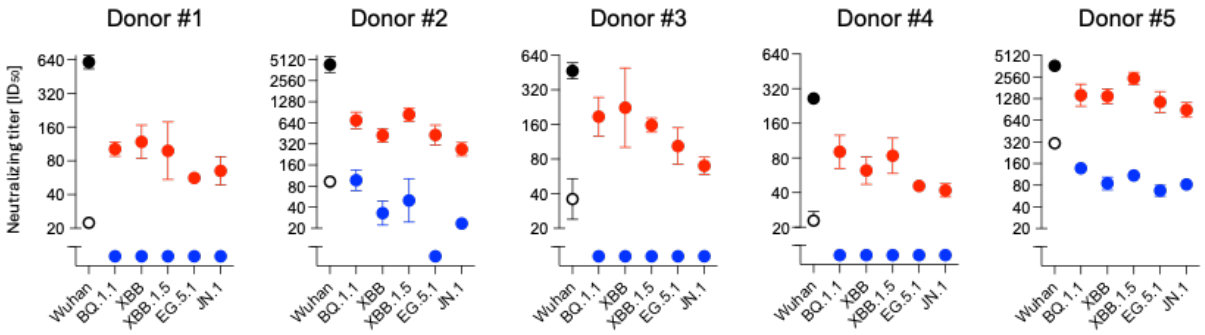


***Figure 2.*** *Neutralization of pseudoviruses carrying different spikes by human sera collected during the pre-Omicron era from persons immunized with original Wuhan-based vaccines. Blue dots indicate neutralization titres against viruses with the indicated native Omicron spikes, whereas red dots mark titres against chimeric viruses carrying the corresponding RBD (residues 330-529) transplanted into Wuhan-D614G backbone. Solid black dots show the titre against a virus with a native Wuhan-D614G spike, whereas empty black dots show the remaining neutralization titre after the same serum was immunodepleted with recombinant RBD protein. Neutralization assays were repeated twice in duplicates. The averages and standard deviations are shown. The original data are provided as a Source Data file.*

In contrast to their poor potency against native Omicron viruses, all five sera could effectively neutralize viruses in which the RBD of these Omicron variants was inserted into the Wuhan-D614G spike backbone, exhibiting $ID_{50}$ titers that were only modestly decreased (~ 2- to 8-fold) against the native Wuhan-D614G virus. Importantly, in all cases, the capacity to neutralize these chimeric viruses was much higher than the residual Wuhan-D614G-neutralizing activity of the same sera after immunodepletion with RBD protein, thereby indicating that there was not a significant contribution of Wuhan-D614G-specific non-RBD-targeting antibodies to neutralization by these sera.

Thus, we conclude that these human sera were rich in antibodies analogous to the six tested bnAb clones by potently targeting RBD epitopes that have remained intact during Omicron evolution but have lost their capacity for potent neutralization because of changes that have occurred elsewhere in the spike protein.

To explore the basis for the selective resistance of Omicron RBDs in their native context, we constructed reciprocal chimeras containing the Wuhan-D614G RBD placed in different Omicron spike backbones. This set of five Wuhan-D614G RBD-containing chimeric spikes covers all but one of the Omicron variants tested in Figure 1, as four of them share the same backbone and differ only in their RBD sequences. When tested against the panel of six bnAbs, the neutralization sensitivity of most of these reciprocal spike chimeras did not significantly differ from Wuhan-D614G (Figure 3A). Together with our earlier results, this finding indicated that the resistant phenotype of the Omicron spike proteins cannot be simply assigned to their RBD domain nor to the remaining spike backbone alone, but instead appears to be determined by the intramolecular dynamics of the entire spike protein.

An interesting exception to the general neutralization sensitivity of the Wuhan-D614G RBD-containing Omicron spike proteins, however, was the chimera 16-C1 composed of the BA.1 spike backbone that was markedly difficult to neutralize by these bnAbs. As a control antibody that does not target a cryptic RBD core epitope, we tested REGN10933 (Casirivimab), a canonical ACE2-competing RBM-binding NAb [28]. It also efficiently neutralized the 16-C1 chimeric spike virus containing the Wuhan-D614G RBD.

This unusual behavior of 16-C1 led us to note that BA.1 spike contains a set of unique mutations in its S2 region that are lacking in subsequent Omicron variants. One of these, namely N856K, is located C-terminally adjacent to the fusion peptide at an interprotomer S1/S2 interface where it could potentially influence molecular interactions within the spike trimer. We therefore tested the effect of introducing the original Wuhan-like asparagine residue into position 856 of the 16-C1 spike. Remarkably, we found that this single back-mutation effectively abolished the bnAb-resistance of 16-C1 (Figure 3).

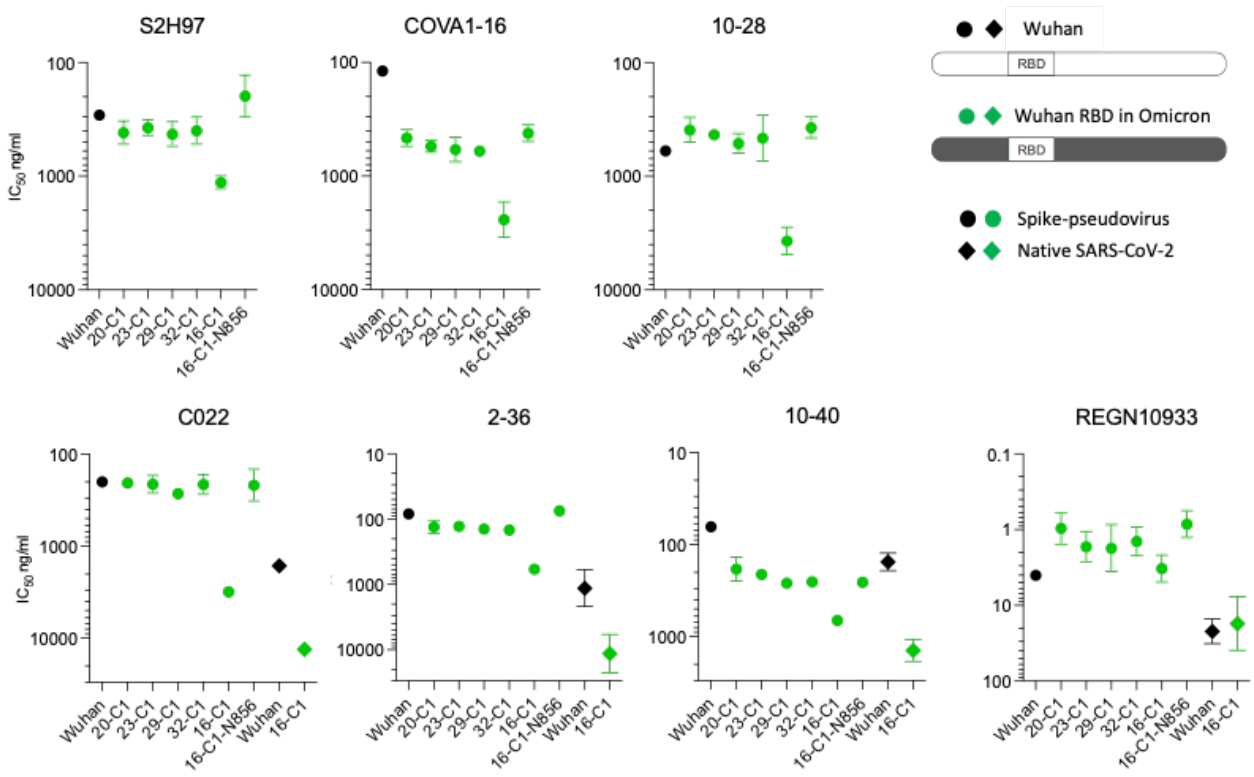


***Figure 3**. Neutralization of pseudoviruses and authentic viruses with chimeric spike proteins by different mAbs. Round symbols indicate neutralization (half-maximal inhibitory mAb concentration) of pseudoviruses containing Wuhan-D614G spike (black dots) or chimeric Omicron spikes containing Wuhan-D614G RBD (green dots). The Omicron backbone of 20-C1 corresponds to the spikes of BA.4/5, BQ.1.1, BF13, and BU.1, whereas 23-C1 is BA.2.75, 29-C1 is XBB, 32-C1 is XBB.1.5, and 16-C1 is BA.1. Data are also shown using a virus pseudotyped with a 16-C1 spike containing a K-to-N back-mutation restoring the Wuhan-like asparagine at position 856. The diamond symbols indicate neutralization of an authentic SARS-CoV-2 virus (Wuhan-D614G; black) and its isogenic recombinant derivative carrying the chimeric BA.1/Wuhan-D614G spike 16-C1 (green). Neutralization assays were repeated independently two or more times in duplicates (pseudoviruses) or triplicates (authentic viruses). The averages and standard deviations of representative assays are shown. The original data are provided in a Source Data file.*

To confirm that target epitope-independent conformational resistance is not restricted to spike-pseudotyped lentiviruses, we used reverse genetics to generate a pair of authentic SARS-CoV-2 viruses to be tested. One of these viruses was based on the Wuhan strain whereas the other was fully isogenic except for carrying the chimeric spike of 16-C1. Recapitulating our results from the pseudovirus model, we found that the SARS-CoV-2 strain carrying 16-C1 spike was much more resistant than the wild-type virus against neutralization by the tested bnAbs that target the cryptic site on RBD, including C022, 2-36, and 10-40, whereas the sensitivity of these viruses for the RBM-targeting control antibody REGN10933 did not differ (Figure 3).

Compared to the prototype SARS-CoV-2 spike, Omicron BA.1 spike trimer has a more tightly packed 3-RBD-down state [29]. We note that residue N856 (K856 in BA.1) is located far from the contacts between the RBD and the rest of the spike and is instead positioned proximal an interprotomer S1/S2 interface (Figure S2). An amino acid change to lysine at this position could contribute to

interprotomer interactions, thereby potentially hindering the opening of the spike trimer, which includes both RBD mobility and the larger scale uncoupling of the trimer subunits during spike "breathing" and its fusogenic conformational transitions [30-33].

On the other hand, because spike trimers of Omicron variants differ from earlier SARS-CoV-2 spikes in favoring a conformation where the three RBDs are in a closed "down-orientation" [29, 34], it could be envisioned that the altered spike dynamics associated with bnAb-resistance would involve impaired access of bnAbs to their cryptic epitopes. To test this possibility, we performed a FACS analysis to compare the ability of our six bnAbs to bind to Wuhan-D614G and 16-C1 spike proteins expressed on the surface of transfected HEK293 cells (Figure 4). However, no substantial difference could be observed in the relative intensity of Wuhan-D614G vs. 16-C1 spike staining by any of these RBD cryptic site binding antibodies. Likewise, we observed that cell surface-expressed neutralization-resistant XBB and EG.5.1 spike proteins were no less brightly stained by these six bNAb than the corresponding spikes comprised of XBB or EG.5.1 RBD domains placed into the Wuhan-D614G backbone. Thus, we conclude that instead of a more restricted target epitope access, these neutralization-resistant spike proteins have evolved to be less prone towards losing their infection-competent prefusion conformation upon bnAb binding.

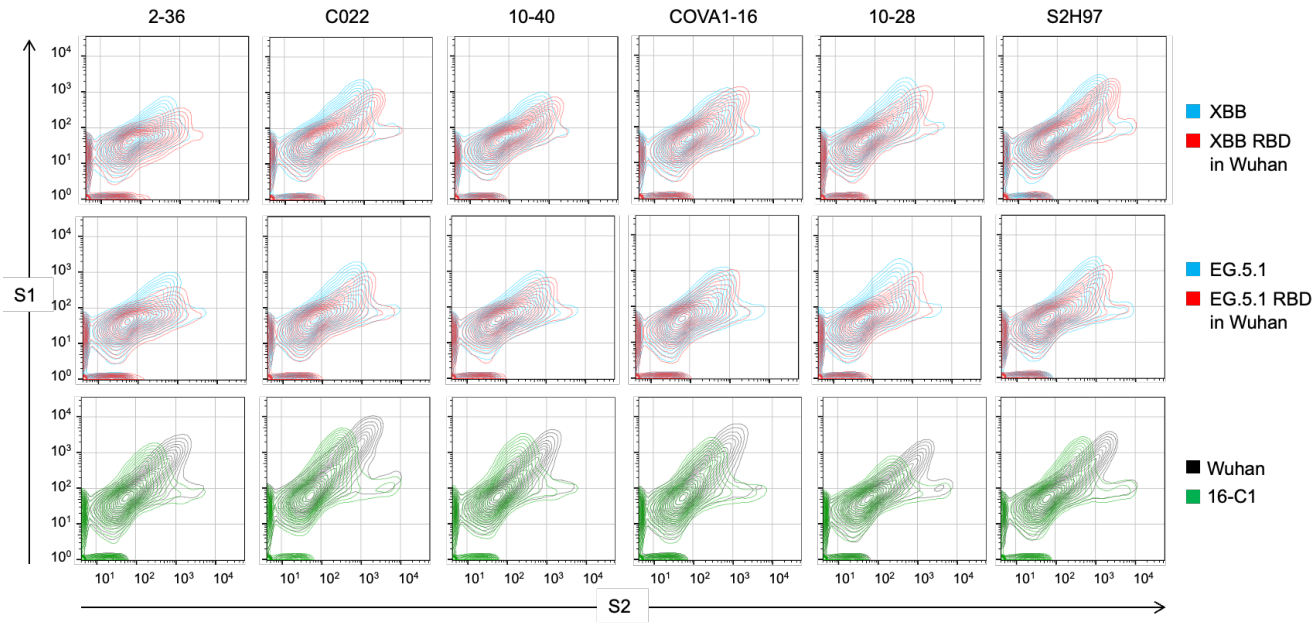


***Figure 4**. FACS analysis of binding to cell surface-expressed spike proteins by bnAbs recognizing cryptic RBD epitopes. Shown are contour plots comparing the staining intensity of spike-transfected cells with the indicated six bnAbs (y-axis) vs. a S2-specific control antibody (x-axis). Each plot shows an overlay of neutralization-sensitive and a neutralization-resistant spike protein pair with identical RBDs.*

## DISCUSSION

Our studies have revealed an unexpected contribution of altered dynamics of the spike protein to the loss of potency of broadly neutralizing human antibodies, thereby amending our understanding of how SARS-CoV-2 evades humoral immunity.

The relative conservation of the cryptic RBD target epitopes of several bnAbs is well-documented, as recently emphasized by Song et al. [35]. However, underlying reasons for the waning potency during the Omicron evolution of neutralizing antibodies targeting highly conserved cryptic RBD epitopes have been overlooked, perhaps because the archetypal members of this class of antibodies (e.g. CR3022 [13]) have been relatively poorly neutralizing compared to RBM antibodies even against the ancestral SARS-CoV-2 strains.

It is therefore noteworthy that a substantial part of the neutralizing activity in the sera of persons immunized in the pre-Omicron era with Wuhan-based vaccines was found to be directed against epitopes that have remained intact in the recent Omicron variants, but lost much of their relevance because of changes in spike dynamics. The magnitude of this conformational immune escape mechanism was surprisingly large. A recent Omicron variant EG.5.1 showed close to complete resistance against neutralization by the tested sera from persons immunized with original Wuhan-based vaccines [36]. Yet, when the spike dynamics were perturbed by transplanting the EG.5.1 RBD to another spike backbone, RBD-targeted antibodies present in these sera could neutralize the virus carrying this chimeric spike with a potency that was only modestly decreased compared to neutralization of a virus with an original Wuhan-D614G spike.

Understanding of the precise molecular mechanism(s) by which SARS-CoV-2 has evolved to protect its infectivity from the action of these antibodies poses an important question for future research. The modes of action of neutralizing antibodies targeting cryptic RBD epitopes are not fully understood but involve destabilization of the spike trimer via differing mechanisms that in some cases may also lead to premature S1 shedding [37-39]. Moreover, despite their non-overlapping RBD binding footprints with ACE2 (see Fig S1), the four YYDxxG antibodies studied here (COVA1-16, 10-40, 2-36, C022) can compete with ACE2 via steric hindrance [14, 18-20]. Consequently, the structural basis for acquired resistance against their effects may also vary.

Restricted access to the cryptic bnAb target epitopes due to a more stable down-conformation of Omicron RBDs[29, 34] could be envisioned to play a role in hindering their action. This conformational stabilization involves hydrophobic substitution of the RBD residue 371 (S371L in BA.1 and S371F in subsequent Omicron variants). In line with these structural considerations, introduction of this single hydrophobic amino acid change into Wuhan-D614G spike has been shown to confer considerable resistance against several neutralizing antibodies from different specificity classes, including 10-40 and REGN10933 used in this study [22, 23]. By contrast, however, we found that when the complete set of RBD mutations of different Omicron variants, including S371L/F, were transferred to the Wuhan-D614G spike backbone, the resulting RBD-chimeric viruses could all be easily neutralized by our panel of bnAbs. Conversely, we found that a F371S back-mutation failed to sensitize native EG.5.1 spike to these antibodies. Thus, we conclude that when present together

with other RBD mutations that have accumulated in the Omicron lineage S371L/F substitution is neither necessary nor predictive for bnAb resistance.

Irrespective of the role of the S371L/F mutation, however, a potential contribution of conformational masking of the cryptic bnAb binding epitopes to neutralization resistance of the Omicron variants remains a relevant question. Our FACS data on comparing surface staining of cells expressing neutralization-resistant or matched sensitive spike proteins (i.e. native Omicrons vs. Wuhan-D614G containing the corresponding RBDs or the chimeric 16-C1 spike vs. Wuhan-D614G) failed to provide support for this model, as cells decorated with resistant spike proteins were stained equally well by these bnAbs as compared to cells with neutralization-sensitive spikes (Figure 4). Therefore, it seems more likely that the conformational resistance of Omicron spikes is due to their increased capacity to maintain a fusion-competent conformation despite bNAb binding.

Some insight into this question was provided by the striking resistance against neutralization by RBD-targeted antibodies of the chimeric spike protein (C16-1) containing the ancestral Wuhan-D614G RBD introduced into the BA.1 backbone. Restoration of a single lysine residue in the S2 region to a Wuhan-like asparagine (K856N) was sufficient to transform C16-1 back to being easy to neutralize. Analysis of available structures of SARS-CoV-2 spike in different conformational states show that residue 856 is distantly located from the contacts between RBD and the rest of the spike (Figure S2) in a position where it may allosterically modulate interprotomeric S1/S2 interactions. The N856K amino acid change could thereby prevent the opening of the spike trimer, which might explain how this residue modulates the neutralization resistance of C16-1 (Figure 3). However, the N856K mutation is unique to BA.1, and placing Wuhan RBD into other Omicron backbones did not give rise to highly resistant viruses. Thus, whereas analogous conformational escape from bnAbs is shared by spike proteins of the Omicron lineage, the underlying molecular details are not identical. Indeed, it has been reported that besides N856K other S2 region mutations shared by most Omicron variants can modulate their fusogenicity and sensitivity to neutralizing antibodies as well as chemical inhibitors of viral entry [40].

The six bnAbs studied here all target epitopes that are not exposed in the RBD-down conformation (see Fig. S1), and their engagement with the spike trimers promotes a 3-RBD-up configuration that is not normally observed in spike structures [14, 16, 18-20]. The RBD displacement imposed by bnAb binding can also be more pronounced than a normal RBD-up conformation, which may further contribute to opening of the spike trimer and destabilization of its prefusion conformation [9, 41, 42] through reduced S1/S2 contacts, leading to the opening of the S2 subunit and separation of monomers from the trimeric stem interface [31-33]. A notable parallel to these observations is provided by the small antibody-mimetic SARS-CoV-2 inhibitor TriSb92 [43]. By targeting a conserved site within the cryptic of Class IV antibody epitope TriSb92 promotes a 3-RBD-up conformation in the spike trimer and triggers structural reorganization of the S2 region to potently block infection without interfering with binding of viral particles to ACE2 expressing cells.

In summary, whereas the details of the intra- and inter-protomer interactions controlling the stability of the spike prefusion conformation remain to be better characterized, it can be concluded that changes in such dynamics underlie the resistance that the Omicron variants have developed against cryptic site-targeting bnAbs. Therefore, to develop more protective SARS-CoV-2 vaccines future immunization strategies should aim at directing the antibody response against spike epitopes that are maximally conserved but yet not critically compromised by this conformational immune escape mechanism. In fact, published data suggest that this might be accomplished at least in part even without elaborate vaccine antigen engineering. As shown by Nussenzweig lab, repeated boosting with the original mRNA-1273 or BNT162b2 vaccines could broaden antibody responses to better cover conserved RBD epitopes and neutralize Omicron BA.1 [44], whereas a recent study on the impact of immunological imprinting by Diamond and colleagues[45] found that further boosting with Omicron-based vaccines elicited neutralizing antibodies with potency also against the XBB.1.5 and EG.5.1 variants as well as more distantly related sarbecoviruses.

## MATERIALS AND METHODS

*Antibody production*

HEK293T cells (ATCC; Catalogue number CRL-3216) were maintained in high-glucose Dulbecco's Modified Eagle Medium (Sigma Aldrich) supplemented with 10% fetal bovine serum, 1% L- Glutamine, and 1% penicillin/streptomycin (complete cell culture medium). The genes encoding the heavy and light chains variable domains of COVA1-16 [18] (7JMX_H and 7JMX_L), 10-28 (7SI2_H and 7SI2_L) [14], 10-40 (7SD5_H and 7SD5_L) [14], 2-36 (7N5H_J and 7N5H_K) [19], C022 (7RKU_J and 7RKU_K) [20], and S2H97 (7M7W_C and 7M7W_D) [16] were ordered as synthetic codon-optimized cDNA fragments (Integrated DNA Technologies), and seamlessly fused using GeneArt Gibson assembly cloning kit (Invitrogen) to the corresponding constant regions (from IgG1 heavy chain allotype IGHG1*01, in the mammalian expression vector pEBB [Addgene 22226]). The heavy and light chain containing vectors were co-transfected into HEK293T cells in complete cell culture medium supplemented with ultra-low IgG FBS (Gibco) using TransIT-2020 reagent (Mirus Bio) according to the manufacturer's instructions. Supernatants containing the secreted human monoclonal antibodies were collected 48-96 h post-transfection, filtered through a 0.2 µm polyethersulfone membrane (Fisherbrand; Catalogue number 15913307), and concentrated using centrifugal filters (Amicon Ultra; catalogue number UFC901008). The final human IgG concentrations were determined using an in house anti-human IgG sandwich-ELISA.

***Pseudoviruses***

HEK293T cells grown in T175 flask were transfected by using TransIT-2020 reagent (Mirus Bio) with the packaging plasmid p8.9NDSB (Addgene #132929), genomic plasmid pWPI (Addgene # 12254) expressing Renilla luciferase, and the expression vector pEBB (Addgene 22226) containing different codon-optimized SARS-CoV-2 spike glycoprotein cDNAs in which the last 18 codons were deleted to enhance the plasma membrane transport. The amino acids sequences for the spike variants used were based on consensus sequences for different SARS-CoV-2 variants according to information from the GISAID initiative (https://gisaid.org) curated by the outbreak.info project [46]. The culture media was replaced 12–16 h post-transfection with complete cell culture medium. The supernatant containing the SARS-CoV-2 spike glycoprotein-harboring pseudoviruses was collected 48 h after transfection and passed through a 0.22µm filter.

***Engineered SARS-CoV-2 strains***

The reverse genetics approach involving five plasmids containing synthetic viral sequence fragments flanked by unique restriction enzyme sites and necessary regulatory sequences for assembling an infectious SARS-CoV-2 cDNA clone based on of the Wuhan-Hu-1 isolate in which a nanoluciferase (NLuc) reporter was placed in-frame after ORF7a protein separated by T2A ribosomal skipping site has been reported elsewhere [47]; the complete confirmed sequence for the successfully rescued virus obtained after transfection of this infection clone into BHK-21 cells can be found in GenBank (MT926412). After modifying the spike-containing plasmid used for infectious cDNA assembly to encode the chimeric spike 16-C1 using PCR and Gibson assembly cloning, the same procedure was repeated to rescue the isogenic virus SARS-CoV-2$^{16\text{-}C1}$. Both viruses were amplified by passaging them in VeroE6-TMPRSS2-H10 cells [48] in viral growth medium (DMEM supplemented with 2% FBS,

1% penicillin-streptomycin, 1% L-glutamine and 25 mM HEPES). The titres of newly reproduced viral stocks were determined by end-point titration, visualized by crystal-violet staining and quantified using a standard Spearmann-Kärber method.

***Neutralization assays***

Pseudovirus neutralization assays were performed essentially as previously described [43]. Briefly, serial dilutions of bNAbs were incubated with SARS-CoV-2 spike pseudotyped lentiviral vectors, after which ACE2-HEK293T cells [43] maintained in complete cell culture medium were added. Productive infection was quantified using Renilla-GLO assay (Promega; catalogue number E2710) and measured using the GloMax Navigator luminometer (Promega, catalogue number GM2010).

Similarly, for neutralization assays with authentic SARS-CoV-2 virus generated using reverse genetics, ACE2-HEK293T cells were seeded on black 96-wells (clear bottom Viewplates; PerkinElmer) in complete cell culture medium 24 h before the assay. Two-fold dilution series of antibodies were prepared in and incubated with an MOI of 0.1 of the two isogenic SARS-CoV-2 strains for 1 h at +37°C. Following the incubation, the complete cell culture medium was removed from the cells and replaced with the antibody + virus mixture-containing media, which after an 1 h infection period was again replaced with viral growth medium after which plates were incubated for another 7 h. Successful infection was quantified using the Nano-GLO Luciferase assay (Promega; Catalogue number N1120) and read on the Hidex Sense microplate reader (Hidex Oy, Finland), using a 3-second capture time. All work done with replication competent viruses was performed under biosafety level 3 conditions.

Half maximal inhibitory concentrations ($IC_{50}$) and half maximal inhibitory dilutions ($ID_{50}$) were determined using Prism10 software (GraphPad). To increase the accuracy of curve fitting, the control value (no antibody added) was set to the average of the measured control value and the values above it in such dilution series where luciferase readings from more than one of wells at the lowest antibody concentrations were higher than in the no-antibody control well.

The human sera used for neutralization assays were collected between September 2021 - January 2022 under informed consent from persons who had received 2 or 3 doses of the BNT162b2 mRNA vaccine with no history of SARS-CoV-2 infection.

***FACS analyses***

HEK293T cells were transfected in 10 cm plates with the same spike-expressing vectors described above for production of spike-containing pseudoviruses. After 68 h, cells were detached by gentle pipetting, washed once with PBS, and suspended in ice-cold FACS buffer (FB; 2 % FBS in PBS). For each staining $1.5x10^5$ cells were incubated on ice for 30 minutes with 1:500 dilution of the mouse anti-S2 Mab 1A9 (Biolegend; catalogue number 944302) and a non-saturating low micromolar concentration of a human anti-S1 bnAb in FB. After three washes with FB, the cells were stained with fluorescently labelled secondary antibodies (goat anti-human IgG Dylight488 from Invitrogen; catalogue number SA5-10134] and goat anti-mouse AlexaFluor647 from Invitrogen; catalogue number A32728], both diluted 1:500 in FB) for 30 min on ice. After washing with FB, the double-stained cells were transferred to FACS tubes and their fluorescence was measured with a flow

cytometer (BD LSR Fortessa; BD Biosciences, USA). The data were analyzed using the FlowJo software (v. 10, BD Sciences).

## DATA AVAILABILITY

All data generated or analysed during this study are included in the main text and its supplementary information files.

## AUTHOR CONTRIBUTIONS

HU and KS designed the study, HU, PS, MY, RF, ARM, AM, TK, IR, IAW and KS analyzed the data., HU, PS, RF, ARM, EZ, TK carried out the laboratory work, MY, IR and IAW did the structural modeling, and PS, MY, RF, ARM, IR, AM, and IAW contributed to writing the manuscript that was drafted by HU and completed by KS.

## ACKNOWLEDGEMENTS

We thank Virpi Syvälahti and Sanna Mäki for expert technical assistance. This work was supported by grants to the Research Council of Finland to KS (331787) and IR (346508) and the Sakari Alhopuro Foundation (02/2021) to KS. Work on SARS-CoV-2 by I.A.W. and M.Y. was supported by a grant from the Bill & Melinda Gates Foundation (INV-004923).

**REFERENCES**


1. WHO Coronavirus (COVID-19) Dashboard. https://covid19.who.int (2024).
2. Markov, P.V. et al. The evolution of SARS-CoV-2. *Nat Rev Microbiol* **21**, 361-369 (2023).
3. Wang, Q. et al. Alarming antibody evasion properties of rising SARS-CoV-2 BQ and XBB subvariants. *Cell* **186**, 279-286.e8 (2023).
4. Cao, Y. et al. BA.2.12.1, BA.4 and BA.5 escape antibodies elicited by Omicron infection. *Nature* **608**, 593-602 (2022).
5. Gruell, H. et al. SARS-CoV-2 Omicron sublineages exhibit distinct antibody escape patterns. *Cell Host Microbe* **30**, 1231-1241.e6 (2022).
6. Cox, M. et al. SARS-CoV-2 variant evasion of monoclonal antibodies based on in vitro studies. *Nat Rev Microbiol* **21**, 112-124 (2023).
7. Miller, J. et al. Substantial neutralization escape by SARS-CoV-2 Omicron variants BQ.1.1 and XBB.1. *N Engl J Med* **388**, 662-664 (2023).
8. He, Q. et al. An updated atlas of antibody evasion by SARS-CoV-2 Omicron sub-variants including BQ.1.1 and XBB. *Cell Rep Med* ***4***, 100991 (2023).
9. Piccoli, L. et al. Mapping neutralizing and immunodominant sites on the SARS-CoV-2 spike receptor-binding domain by structure-guided high-resolution serology. *Cell* **183**, 1024-1042.e21 (2020).
10. Premkumar, L. et al. The receptor binding domain of the viral spike protein is an immunodominant and highly specific target of antibodies in SARS-CoV-2 patients. *Sci Immunol* **5**, eabc8413 (2020).
11. He, W.T. et al. Targeted isolation of diverse human protective broadly neutralizing antibodies against SARS-like viruses. *Nat Immunol* **23**, 960-970 (2022).
12. Pinto, D. et al. Cross-neutralization of SARS-CoV-2 by a human monoclonal SARS-CoV antibody. *Nature* **583**, 290-295 (2020).
13. Yuan, M. et al. A highly conserved cryptic epitope in the receptor binding domains of SARS-CoV-2 and SARS-CoV. *Science* **368**, 630-633 (2020).
14. Liu, L. et al. An antibody class with a common CDRH3 motif broadly neutralizes sarbecoviruses. *Sci Transl Med* **14**, eabn6859 (2022).
15. Wu, N.C. et al. A natural mutation between SARS-CoV-2 and SARS-CoV determines neutralization by a cross-reactive antibody. *PLoS Pathog* **16**, e1009089 (2020).
16. Starr, T.N. et al. SARS-CoV-2 RBD antibodies that maximize breadth and resistance to escape. *Nature* **597**, 97-102 (2021).
17. Greaney, A.J. et al. Complete mapping of mutations to the SARS-CoV-2 spike receptor-binding domain that escape antibody recognition. *Cell Host Microbe* **29**, 44-57.e49 (2021).
18. Liu, H. et al. Cross-neutralization of a SARS-CoV-2 antibody to a functionally conserved site is mediated by avidity. *Immunity* **53**, 1272-1280 e1275 (2020).
19. Wang, P. et al. A monoclonal antibody that neutralizes SARS-CoV-2 variants, SARS-CoV, and other sarbecoviruses. *Emerg Microbes Infect* **11**, 147-157 (2022).
20. Jette, C.A. et al. Broad cross-reactivity across sarbecoviruses exhibited by a subset of COVID-19 donor-derived neutralizing antibodies. *Cell Rep* **36**, 109760 (2021).

21. Cao, Y. et al. Omicron escapes the majority of existing SARS-CoV-2 neutralizing antibodies. *Nature* **602**, 657-663 (2022).
22. Iketani, S. et al. Antibody evasion properties of SARS-CoV-2 Omicron sublineages. *Nature* **604**, 553-556 (2022).
23. Liu, L. et al. Striking antibody evasion manifested by the Omicron variant of SARS-CoV-2. *Nature* **602**, 676-681 (2022).
24. Zhang, J. et al. Structural and functional impact by SARS-CoV-2 Omicron spike mutations. *Cell Rep* **39**, 110729 (2022).
25. Addetia, A. et al. Neutralization, effector function and immune imprinting of Omicron variants. *Nature* **621**, 592-601 (2023).
26. Kurhade, C. et al. Low neutralization of SARS-CoV-2 Omicron BA.2.75.2, BQ.1.1 and XBB.1 by parental mRNA vaccine or a BA.5 bivalent booster. *Nat Med* **29**, 344-347 (2023).
27. Wang, Q. et al. Antibody neutralisation of emerging SARS-CoV-2 subvariants: EG.5.1 and XBC.1.6. *Lancet Infect Dis* **23**, e397-e398 (2023).
28. Baum, A. et al. Antibody cocktail to SARS-CoV-2 spike protein prevents rapid mutational escape seen with individual antibodies. *Science* **369**, 1014-1018 (2020).
29. Gobeil, S.M. et al. Structural diversity of the SARS-CoV-2 Omicron spike. *Mol Cell* **82**, 2050-2068 e2056 (2022).
30. Fukuhara, H. et al. Unprecedented spike flexibility revealed by BSL3 Cryo-ET of active SARS-CoV-2 virions. *bioRxiv* **doi: https://doi.org/10.1101/2023.10.10.561643** (2023).
31. Olmedillas, E. et al. Structure of a SARS-CoV-2 spike S2 subunit in a pre-fusion, open conformation. *bioRxiv* **doi: https://doi.org/10.1101/2023.12.14.571764** (2023).
32. Costello, S.M. et al. The SARS-CoV-2 spike reversibly samples an open-trimer conformation exposing novel epitopes. *Nat Struct Mol Biol* **29**, 229-238 (2022).
33. Zimmerman, M.I. et al. SARS-CoV-2 simulations go exascale to predict dramatic spike opening and cryptic pockets across the proteome. *Nat Chem* **13**, 651-659 (2021).
34. Stalls, V. et al. Cryo-EM structures of SARS-CoV-2 Omicron BA.2 spike. *Cell Rep* **39**, 111009 (2022).
35. Song, G. et al. Broadly neutralizing antibodies targeting a conserved silent face of spike RBD resist extreme SARS-CoV-2 antigenic drift. *bioRxiv* (2023).
36. Polack, F.P. et al. Safety and Efficacy of the BNT162b2 mRNA Covid-19 Vaccine. *N Engl J Med* **383**, 2603-2615 (2020).
37. Liu, H. & Wilson, I.A. Protective neutralizing epitopes in SARS-CoV-2. *Immunol Rev* **310**, 76-92 (2022).
38. Huang, Q., Han, X. & Yan, J. Structure-based neutralizing mechanisms for SARS-CoV-2 antibodies. *Emerg Microbes Infect* **11**, 2412-2422 (2022).
39. Errico, J.M., Adams, L.J. & Fremont, D.H. Antibody-mediated immunity to SARS-CoV-2 spike. *Adv Immunol* **154**, 1-69 (2022).
40. Kumar, S. et al. Mutations in S2 subunit of SARS-CoV-2 Omicron spike strongly influence its conformation, fusogenicity, and neutralization sensitivity. *J Virol* **97**, e0092223 (2023).

41. Huang, K.A. et al. Structural basis for a conserved neutralization epitope on the receptor-binding domain of SARS-CoV-2. *Nat Commun* **14**, 311 (2023).
42. Zhou, D. et al. Structural basis for the neutralization of SARS-CoV-2 by an antibody from a convalescent patient. *Nat Struct Mol Biol* **27**, 950-958 (2020).
43. Mäkelä, A.R. et al. Intranasal trimeric sherpabody inhibits SARS-CoV-2 including recent immunoevasive Omicron subvariants. *Nat Commun* **14**, 1637 (2023).
44. Muecksch, F. et al. Increased memory B cell potency and breadth after a SARS-CoV-2 mRNA boost. *Nature* **607**, 128-134 (2022).
45. Liang, C.Y. et al. Imprinting of serum neutralizing antibodies by Wuhan-1 mRNA vaccines. *Nature* **630**, 950-960 (2024).
46. Gangavarapu, K. et al. Outbreak.info genomic reports: scalable and dynamic surveillance of SARS-CoV-2 variants and mutations. *Nat Methods* **20**, 512-522 (2023).
47. Rihn, S.J. et al. A plasmid DNA-launched SARS-CoV-2 reverse genetics system and coronavirus toolkit for COVID-19 research. *PLoS Biol* **19**, e3001091 (2021).
48. Rusanen, J. et al. A generic, scalable, and rapid time-resolved Förster resonance energy transfer-based assay for antigen detection-SARS-CoV-2 as a proof of concept. *mBio* **12**, e00902-00921 (2021).
49. Xiong, X. et al. A thermostable, closed SARS-CoV-2 spike protein trimer. *Nat Struct Mol Biol* **27**, 934-941 (2020).
50. Hansen, J. et al. Studies in humanized mice and convalescent humans yield a SARS-CoV-2 antibody cocktail. *Science* **369**, 1010-1014 (2020).
51. Krissinel, E. & Henrick, K. Inference of macromolecular assemblies from crystalline state. *J Mol Biol* **372**, 774-797 (2007).
52. Goddard, T.D. et al. UCSF ChimeraX: Meeting modern challenges in visualization and analysis. *Protein Sci* **27**, 14-25 (2018).
53. Pettersen, E.F. et al. UCSF ChimeraX: Structure visualization for researchers, educators, and developers. *Protein Sci* **30**, 70-82 (2021).

**SUPPLEMENTARY DATA**

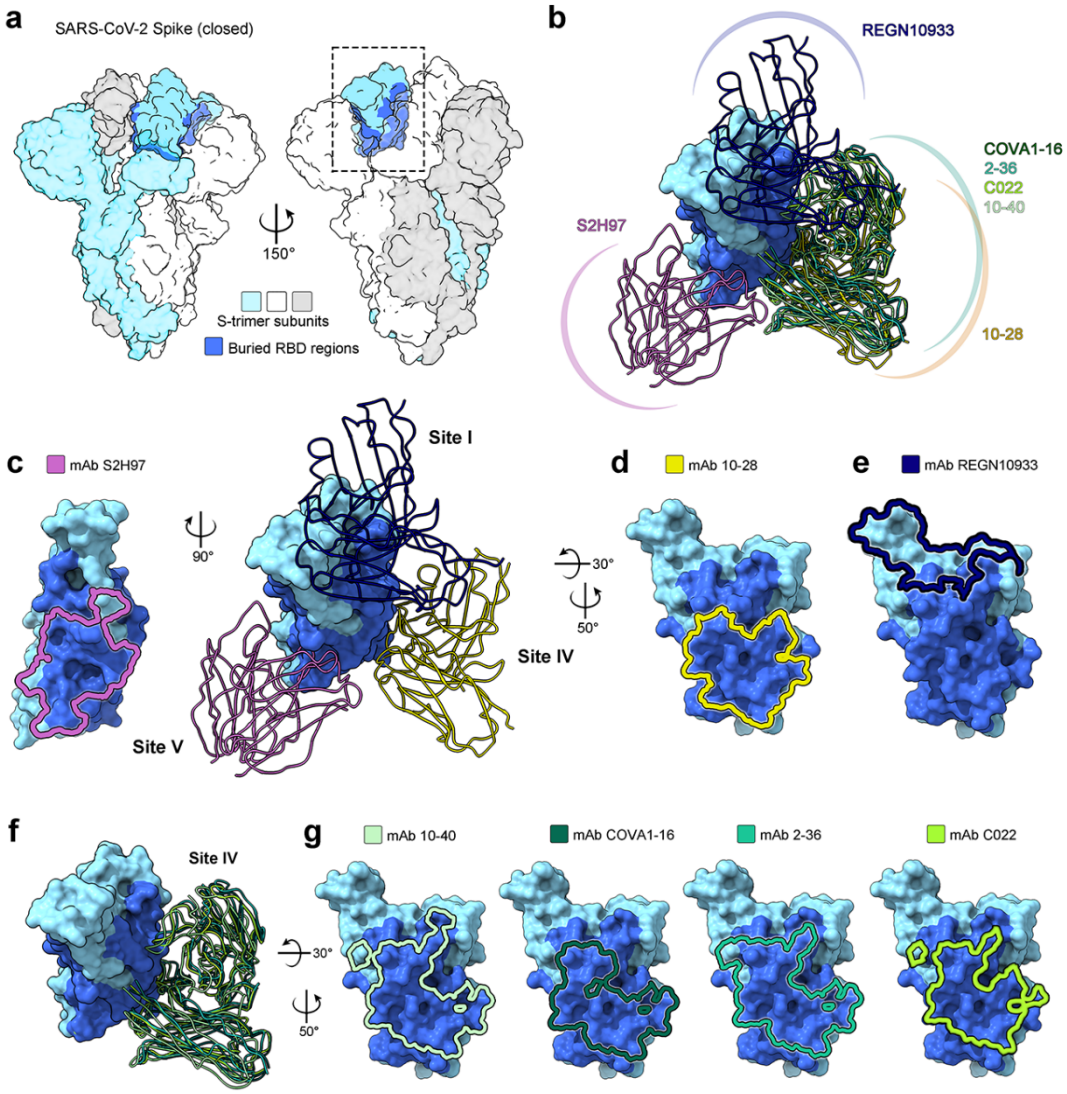


**Figure S1.** The epitopes targeted by the neutralizing antibodies (nAbs) used in this study. **a.** A surface representation of the SARS-CoV-2 S-trimer (PDB 6ZP0 [49]). The trimer subunits are shown in white, grey, and light blue, with the regions of the receptor-binding domain (RBD) that are inaccessible when the RBD is in the "down" or "closed" conformation highlighted in dark blue on one subunit. **b.** The antibodies examined in this study, namely COVA1-16 [18], 10-28 [14], 10-40 [14], 2-36 [19], C022 [20], and S2H97 [16], all bind regions of RBD that are buried in the down state. The epitope of mAb REGN10933 (Casirivimab) [28, 50], which targets the ACE2-binding site, is shown for comparison. **c-e.** The binding modes and epitopes of mAb S2H97 (PDB 7M7W), 10-28 (PDB 7SI2) and REGN10933 (PDB 6XDG), which target antigenic sites V, IV and I, respectively. **f-g.** The binding modes and epitopes of mAbs COVA1-16 (PDB 7JMW), 10-40 (PDB 7SD5), 2-36 (PDB 7N5H), and C022 (PDB 7RKU), which target antigenic site IV. Epitope residues for each antibody-RBD complex were determined by the PDBePISA [51] tool for the exploration of macromolecular interfaces, and molecular graphics were generated with UCSF ChimeraX [52, 53]. For clarity, only the Fv region of each antibody is shown, and all epitopes are shown mapped on the RBD from the S-trimer structure (PDB 6ZP0) [49].

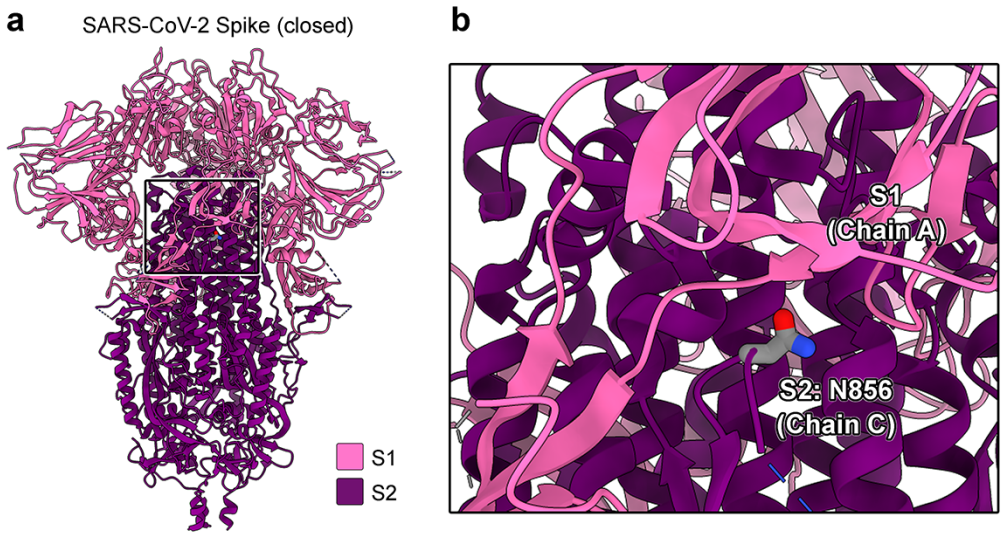


**Figure S2.** Residue N856 (K856 in BA.1) within SARS-CoV-2 S-trimer S2 is located at an inter-subunit interface. **a.** A cartoon representation of the SARS-CoV-2 S-trimer (PDB 6ZP0 [49]). The trimer subunits are colored pink for the S1 region (residues up to 667) and dark purple for the S2 region (residues 668 and beyond). **b.** A close-up panel displaying N856 in stick representation. Molecular graphics were generated with UCSF ChimeraX [28, 50].